Alexandria Engineering Journal (2017) 56, 241–249

HOSTED BY

ELSEVIER

Alexandria University

Alexandria Engineering Journal

www.elsevier.com/locate/aej
www.sciencedirect.com

ORIGINAL ARTICLE

Seismic performance of steel frames designed using different allowable story drift limits

Hamdy Abou-Elfath *, **Mostafa Ramadan**, **Mohamed Meshaly**, **Heba Alzobair Fdiel**

Structural Eng. Dept., Faculty of Engineering, Alexandria University, Alexandria, Egypt

Received 17 July 2016; accepted 28 August 2016
Available online 9 September 2016

KEYWORDS

Steel frame;
Story drift;
Earthquake;
Pushover;
Seismic damage;
Performance evaluation

Abstract The design of Moment Resisting Steel Frames (MRSFs) is usually governed by drift limits rather than strength because of their high flexibility. The purpose of this study is to evaluate the seismic performance of a 6-story MRSF designed according to the Egyptian code with three different levels of allowable story drift limits: 0.5%, 0.75% and 1.0%. Seismic evaluation in this study has been carried out by static pushover analysis and time history earthquake analysis. Ten ground motions with different PGA levels are used in the analysis. The mean plus one standard deviation values of the roof-drift ratio, the maximum story drift ratio and the maximum beam- and column-strain responses are used as the basis for the seismic performance evaluations.

The results obtained indicated that the strength and the initial stiffness of the designed frames decrease as the allowed story drift limit of the frame increases. Two of the designed frames exhibit maximum story drifts that are higher than the allowed limits specified by the code. The maximum story drift and beam-strain responses of the designed frames under the earthquake loading increase with the increase in the allowable story drift limits.

1. Introduction

The main objective of seismic codes including the recent Egyptian code (ECP-201) [1] is to achieve satisfactory performance of structural systems when subjected to earthquake loading. However, seismic design of building structures is usually conducted by approximate procedures that rely on using elastic static analysis instead of the actual inelastic dynamic one. This highlights the importance of evaluating the actual dynamic inelastic performance of the code designed structures under the effect of real earthquake records. Such evaluation is essential to provide information on the level of protection afforded to the code designed structures against seismic loading.

The Egyptian code provisions for the seismic design of MRSFs have been evaluated through parametric and comparative investigations using different analysis procedures and numerical models. The analysis has been conducted at either the structure-level or the beam-to-column connection level. Shehata et al. [2] analyzed MRSFs designed according to the Egyptian code with strong and weak-joint approaches. The global and local performance parameters of the frames are evaluated under lateral loading conditions. The results indicated satisfactory performance of both the design approaches. Serror et al. [3] investigated how to define the boundary between special moment resisting frame and ordinary moment

* Corresponding author.
E-mail address: Hamdyabou@yahoo.com (H. Abou-Elfath).

Peer review under responsibility of Faculty of Engineering, Alexandria University.

http://dx.doi.org/10.1016/j.aej.2016.08.028
1110-0168 © 2016 Faculty of Engineering, Alexandria University. Production and hosting by Elsevier B.V.

resisting frame in the ECP-201. The seismic provisions of ECP-201 have been compared with those of the Euro-Code 8 and the Uniform Building Code with regard to ductility classes and their impact on the response modification factor. They suggested specifying a structure as special moment resisting frame means that its members should adhere to class 1 (compact width-to-thickness ratio) requirements; while specifying a structure as ordinary moment resisting frame means that using members of class 2 (non-compact/slender width-to-thickness ratio) is permitted.

Finite element modeling of MRSF connections has been conducted by Mashaly et al. [4,5]. The software package ANSYS is used to model the joint under the effect of lateral loading. The results confirmed that the chosen parameters such as material and section geometry of the joint, played effective roles on the energy dissipation of the connection under seismic loading.

El-Shaer [6] evaluated the effect of earthquake on steel frames with partial rigid connection. The analysis was based on the nonlinear dynamic analysis considering both geometrical and material nonlinearities. The analysis demonstrated that the calculated displacement responses are close to those proposed by different seismic codes. Abdel Raheem [7] evaluated the Egyptian code provisions for the seismic design of moment-resistant frame multi-story building through using nonlinear time history analysis, equivalent static load and response spectrum analysis methods. He found that diaphragm flexibility caused an increase in the fundamental period and in floor displacements compared with the case of rigid diaphragms of equivalent buildings. He concluded that the code empirical methods under-predict the fundamental period of structures with flexible diaphragms. He also concluded that the equivalent static force approach of the ECP-201 is not accurate as it overestimates the base shear. Serror and Abdelmoneam [8] evaluated the performance of MRSFs designed according to the Egyptian code. The focus of their study was on the effect of beam slenderness limit on the anticipated ductility of MRSFs. They proposed guidelines to estimate the appropriate force reduction factor, R-factor, based on the beam slenderness limit.

Most recent seismic codes, including the Egyptian code for calculating loads (ECP-201) are developed with two performance levels. One, with the intent of limiting damage during frequent moderate earthquakes namely the serviceability limit state and the other is for ensuring collapse prevention during a major earthquake namely the ultimate limit state [9]. Displacement parameters often offer better evaluation of damage effects than force parameters when assessing structures to a serviceability limit state [10]. Therefore limiting displacement is a requirement for controlling the seismic damage.

In order to estimate the actual inelastic displacement that develops in strong earthquakes, ECP-201 specifies that the computed displacement from the reduced lateral forces is amplified by a factor that is equal to $0.7 \times$ R-factor. The R-factor is the force reduction factor that accounts for the ductile inelastic behavior of the structural system. For the case of moderate frequent earthquake, the displacement demand is estimated by reducing the strong-earthquake displacement to account for the difference in return periods between the strong earthquake and the frequent one. ECP-201 uses a displacement reduction factor v for this purpose. The value of the displacement reduction factor v is 0.4 for important structures and 0.5 for ordinary buildings.

Seismic codes specify limits on the lateral displacement demand corresponding to moderate frequent earthquakes to control seismic damage to nonstructural components for serviceability considerations. Traditionally lateral displacement has been defined in terms of story drift which is the relative lateral displacement occurring between two successive floors. Limitations on story drift ratios vary among the codes, generally ranging from 0.25% to 1.5% depending on the type of the non-structural elements. The Egyptian code specifies three levels of allowable story drift limit depending on the type of the non-structural elements and their arrangements into the structure. The code specifies 0.5% allowable story drift ratio for brittle partitions, 0.75% for ductile partitions and 1.0% for structural systems with partitions fully isolated from the structure motion.

The objective of this study is to evaluate the seismic performances of a 6-story MRSF designed according to the Egyptian code with different levels of allowable story drift limits. Three design cases of the 6-story MRSFs, D_1, D_2, and D_3 are considered in this study. These design cases are corresponding to allowable story drift limits of 0.5, 0.75, and 1.0%, respectively. Seismic evaluation in this study has been carried out using static pushover analysis and time history earthquake analysis using the SeismoStruct computer program [11]. Ten ground motions with different PGA levels are used in the analysis. Each of the ground motion records is scaled to different PGA levels to excite the structure well into the inelastic range of deformation. The mean plus one standard deviation values of the roof-drift ratio, the maximum story drift ratio and the maximum beam- and column-strain responses are used as the basis for the seismic performance evaluations.

2. Prototype frames and computer program

The prototype steel building considered in this study is a 6-story office building located in Cairo, Egypt with a design PGA of 0.15 g. The plan of the building, shown in Fig. 1, has a rectangular configuration with 5-bays in the short direction and 7-bays in the long direction. The bay width in both directions is constant and equals to 7.5 m. The story height is 4.5 m for the ground floor and 3.5 m for other floors with the total building height of 22.0 m. The floors consist of 10 cm light weight concrete slab over a composite metal deck. Structural members are selected from the American wide flange sections (W-sections). The usual structural steel specification for W-sections is ASTM A992. The yield strength is 345 MPa, modulus of elasticity is 200 GPa, strain hardening ratio is 0.01, and the shear modulus is 81 GPa.

The building is considered to have MRSFs in the perimeter of the short direction and braced steel frames in the perimeter of the long direction to carry the seismic loads. A typical perimeter MRSF in the short direction is shown in Fig. 2. The dead load is assumed equal to 5 kPa and it includes weights of deck, beams, girders, ceiling, partitions and mechanical and electrical systems. Surface weight of the exterior walls is considered equal to 1.25 kPa. The applied live load considered is taken 3 kPa for office buildings.

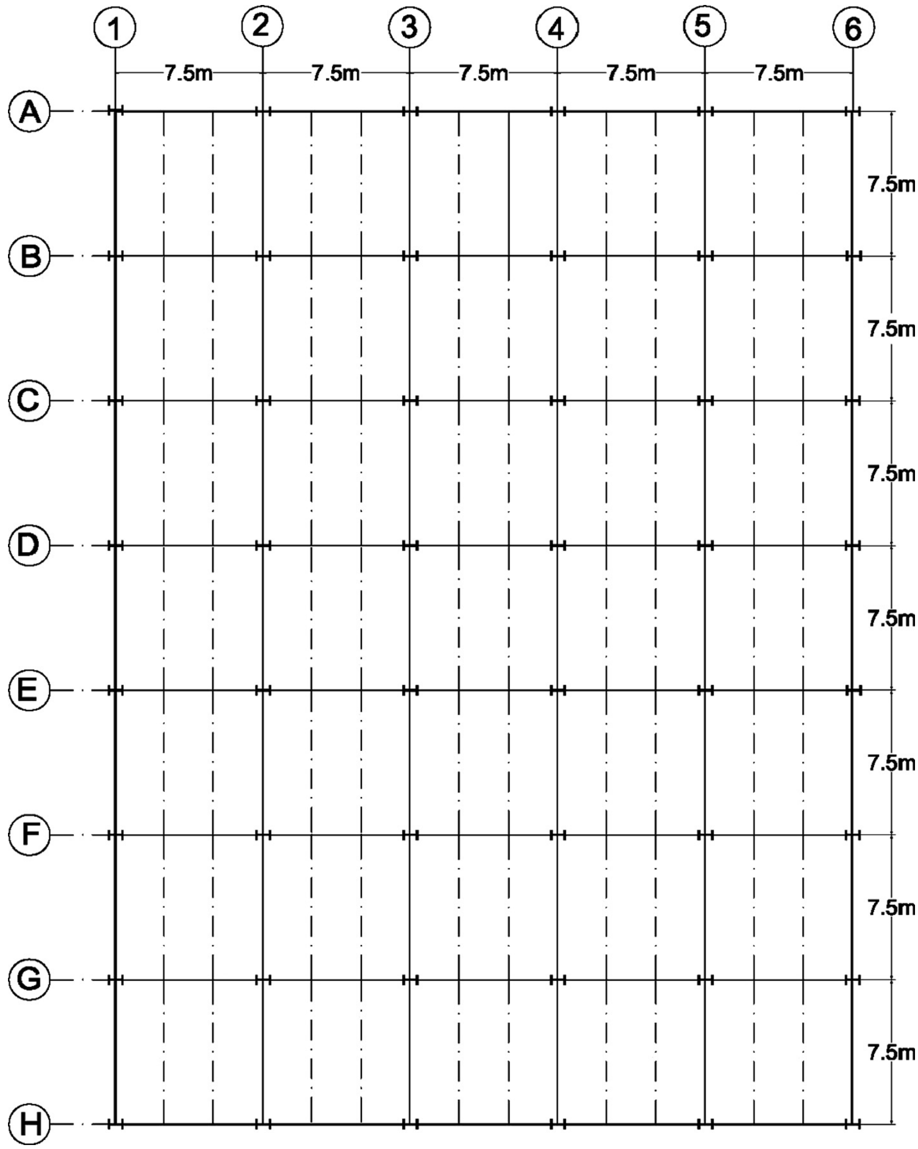

Figure 1 Floor plan view of the steel office building.

The MRSF design has been performed in accordance with the Egyptian codes ECP-201 and ECP-205 [12]. The design internal forces are calculated by considering the critical combination of gravity and seismic or wind loading. The frame is considered to have adequate-ductility with R-factor of 7. Beams and columns have been designed using compact rolled sections. This has been accomplished by applying the code requirements for local buckling requirements of webs and flanges of the cross sections. The code requirements for preventing the panel zone yielding and for the strong-column weak-beam design have also been applied.

Drift checks have been performed based on the code limits. ECP-201 specifies that the computed displacement from the reduced lateral forces is amplified by a factor that is equal to $0.7 \times$ R-factor. For the case of moderate frequent earthquake, the displacement demand is estimated by reducing the strong-earthquake displacement to account for the difference in return periods between the strong earthquake and the frequent one. ECP-201 uses a displacement reduction factor v for this purpose. The value of the displacement reduction factor v is 0.4 for important structures and 0.5 for ordinary buildings.

The Egyptian code specifies three levels of allowable story drift limit depending on the type of the non-structural elements and their arrangements into the structure. The code specifies 0.5% allowable story drift ratio for brittle partitions, 0.75% for ductile partitions and 1.0% for structural systems with partitions fully isolated from the structure motion.

Three design cases of the 6-story MRSF, D_1, D_2, and D_3 are considered in this study. These design cases are corresponding to allowable story drift limits of 0.5, 0.75, and 1.0%, respectively. The sizes of the columns and beams cross sections are summarized in Table 1 for the three design cases. The frames were modeled using the SeismoStruct computer program [11]. Beams and columns are modeled using the force-based beam-column element that utilizes the fiber modeling approach to capture the spread of inelasticity along the

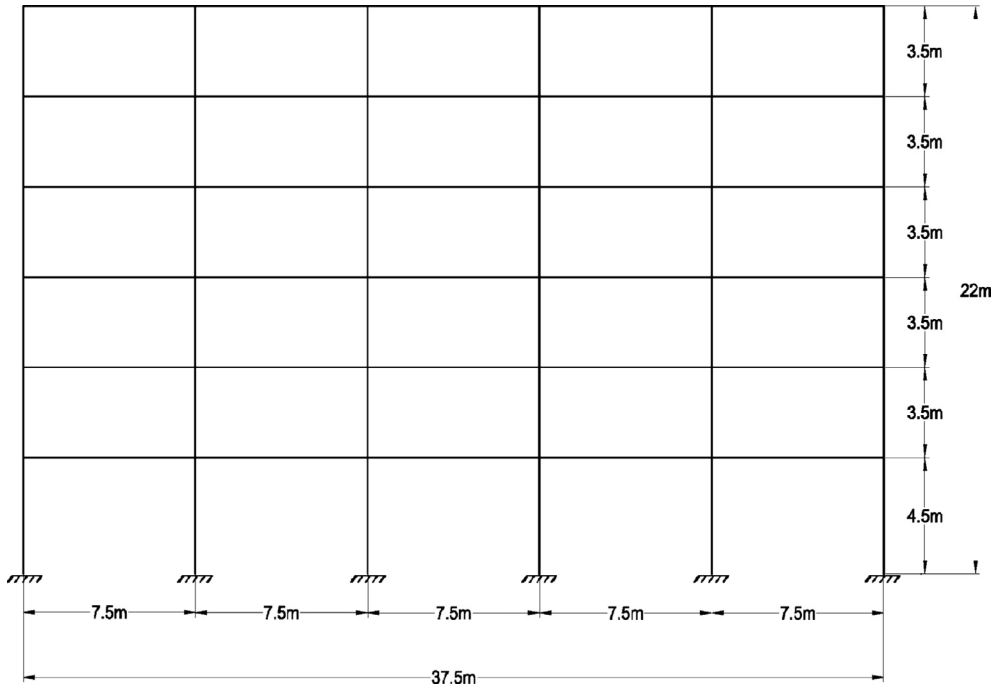

Figure 2 Elevation view of the MRSF.

Table 1 Cross section details of the MRSF design cases.

Story	Beams	Exterior column	Interior column
Case D_1			
1	W30 × 116	W14 × 193	W14 × 311
2	W30 × 108	W14 × 159	W14 × 257
3	W30 × 99	W14 × 132	W14 × 257
4	W27 × 84	W14 × 120	W14 × 211
5	W21 × 68	W14 × 109	W14 × 159
6	W21 × 44	W14 × 43	W14 × 109
Case D_2			
1	W30 × 90	W14 × 159	W14 × 257
2	W30 × 90	W14 × 120	W14 × 233
3	W24 × 84	W14 × 120	W14 × 193
4	W24 × 68	W14 × 82	W14 × 145
5	W21 × 55	W14 × 68	W14 × 132
6	W16 × 40	W14 × 43	W14 × 61
Case D_3			
1	W24 × 76	W14 × 120	W14 × 176
2	W24 × 76	W14 × 109	W14 × 159
3	W24 × 62	W14 × 109	W14 × 159
4	W24 × 55	W14 × 68	W14 × 120
5	W21 × 44	W14 × 53	W14 × 109
6	W18 × 35	W14 × 34	W14 × 61

member length. The member is subdivided into segments distributed along the member length, and the cross section of each segment is subdivided into steel fibers. A uniaxial bilinear stress-strain model with kinematic strain hardening is assigned for each fiber. The sectional stress-strain state is obtained through the integration of the nonlinear uniaxial stress-strain response of the individual fibers forming the cross-section while the member response is obtained by integrating sectional responses along the member length.

3. Pushover static analysis

The results of the pushover analysis obtained using the SeismoStruct computer program provide information on the load-displacement relationships of the roof level and the various stories of the structure. The distributions of the story displacements obtained from the pushover analysis are very important in evaluating the overall ductility of the structure. Also, local deformations of the structure elements obtained from the pushover analysis are important in determining the critical elements in the structure.

Pushover analysis is conducted up to 2% roof drift ratio using the lateral load distribution pattern specified in the Egyptian code. Gravity loads are applied on the frame during the pushover analysis and is considered equal to the dead loads plus half of the live loads.

Fig. 3 shows the relationships between the base-shear coefficient and the roof drift ratios of the three design cases of the 6-story frame. The base-shear coefficient is defined as the base shear divided by the building weight. The results shown in Fig. 3 indicate that the strength and the initial stiffness decrease as the allowed story drift limit of the frame increases. For the three design cases D_1, D_2, and D_3, the ultimate base shear coefficients are equal to 0.166, 0.124 and 0.087, respectively and the over strength factors, Ω, are equal to 5.53, 4.13, and 2.9, respectively.

Fig. 4 shows the distributions of story drift ratios along the frame height corresponding to 2.0% roof drift ratio. The maximum story drift ratios of the three design cases D_1, D_2, and D_3 reached 2.37, 2.05, and 2.28%, respectively. This indicates that the design case D_2 has the best deformability among all the design cases.

The column and beam strain factor is defined as the maximum strain in column or beam divided by the yield strain of

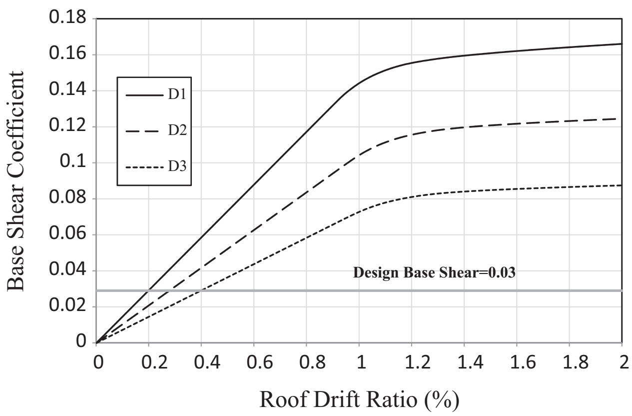

Figure 3 Relationships between the base shear coefficient and the roof drift ratio of the three design cases.

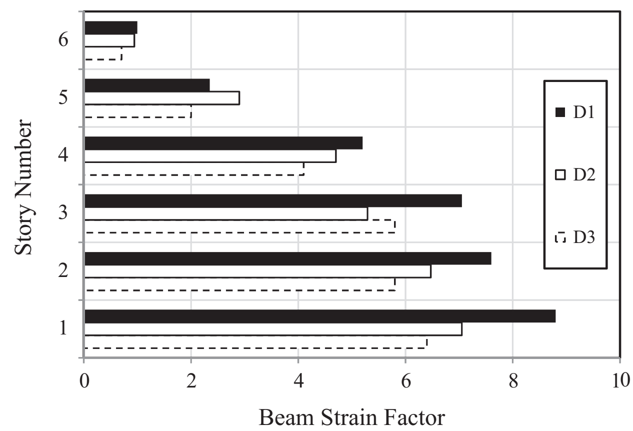

Figure 5 Height-wise distribution of beam strain factors at 2.0% roof drift ratio.

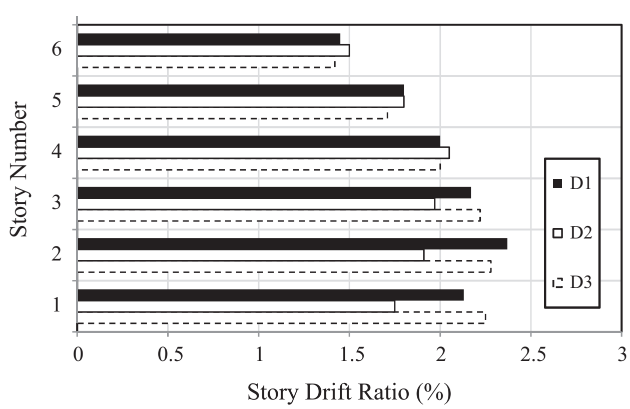

Figure 4 Height-wise distribution of story drift ratios of the three design cases at 2.0% roof drift ratio.

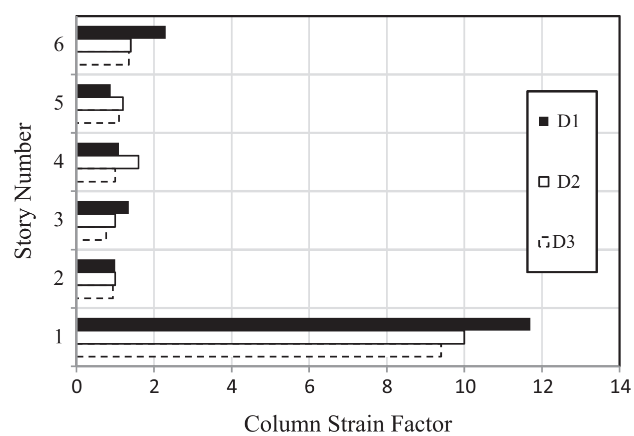

Figure 6 Height-wise distribution of column strain factors at 2.0% roof drift ratio.

steel ($\varepsilon_y = 0.0017$). The distribution of maximum strain factors along the frame stories corresponding to 2.0% roof drift ratios is shown in Fig. 5 for beams and Fig. 6 for columns. For the three design cases D_1, D_2, and D_3, the maximum beam strain factors occurred in the first story and reached 8.8, 7.05, and 6.4%, respectively, and the maximum column strain factors occurred also in the first story and reached 11.7, 10, and 9.4%, respectively. These results show that the design case D_1 exhibited the highest levels of beam and column strains, while case D_3 showed the lowest levels of beam and column strains. This indicates that at any specific roof drift ratio, the higher the allowable story drift limit is, the lower is the maximum strains in columns and beams.

4. Fundamental periods of the designed MRSFs

The fundamental periods of the designed MRSFs calculated by the SeismoStruct computer program are 1.87, 2.2 and 2.67 s for the design cases D_1, D_2 and D_3, respectively. The fundamental periods of the D_2 and D_3 design cases are 17.7%, and 42.8% higher than the D_1 design case. These results indicate that the fundamental period of the frame increases with the increase in the allowable story drift limit. The fundamental period of the frames calculated by the ECP-201 equation ($T = Ct\ H^{3/4}$) is equal to 0.86 s. It can be observed that the exact fundamental periods of the frames are much longer than the values suggested by ECP-201. The code equation is empirical and its value is expected to be in the safe side. In other words, the code prediction has to be lesser than the exact values calculated from the exact analysis.

5. Earthquake response of the MRSFs

The earthquake analysis of the MRSFs is performed using a time step increment of 0.005 s and Rayleigh damping which is defined to achieve 5.0% viscous damping in the first two natural modes of the building. Ten ground motions with different PGA levels are used in the analysis. The Earthquake data and site information for the selected ground motions records are presented in Table 2.

The seismic performances of the investigated MRSFs are assessed using four performance parameters which include the roof drift ratio, the maximum story drift ratio, the maxi-

Table 2 Earthquake data and site information for the selected ground motions.

Record no	Event	Year	Record station	Φ[1]	M^{*2}	R^{*3} (km)	PGA (g)
1	Imperial Valley	1979	Cucapah	85	6.9	23.6	0.309
2	Loma Prieta	1989	Anderson Dam	270	6.9	21.4	0.244
3	Imperial Valley	1979	Chihuahua	282	6.5	28.7	0.254
4	Imperial Valley	1979	El Centro Array # 13	230	6.5	21.9	0.139
5	Imperial Valley	1979	El Centro Array # 13	140	6.5	21.9	0.117
6	Superstition Hill	1987	Wildlife Liquefaction Array	360	6.7	24.4	0.2
7	Loma Prieta	1989	Holister South & Pine	0	6.9	28.8	0.371
8	Superstition Hill	1987	Wildlife Liquefaction Array	90	6.5	24.4	0.18
9	Loma Prieta	1989	Sunnyvale Colton Ave	360	6.9	28.8	0.209
10	Loma Prieta	1989	Waho	90	6.9	16.9	0.638

Φ[1] the component, M^{*2} the moment magnitudes, R^{*3} closest distances to fault rupture.

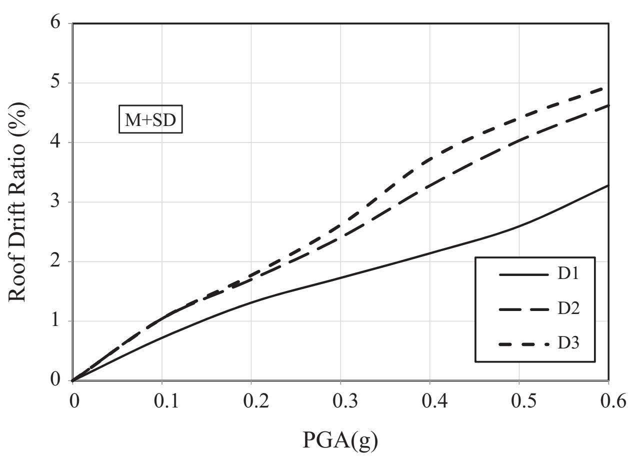

Figure 7 Relationships between the (M + SD) roof-drift-ratios and the PGA of the earthquakes.

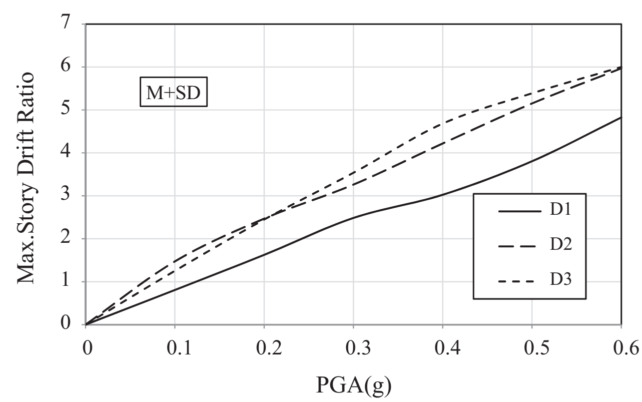

Figure 8 Relationships between the (M + SD) maximum story drift ratios and the PGA of the earthquakes.

mum column strain response and the maximum beam strain response. The mean plus one standard deviation (M + SD) values of the performance parameters are used as the basis for the seismic performance evaluations.

Fig. 7 shows the relationships between the (M + SD) roof drift ratios and the PGA of the earthquakes. The results presented in Fig. 7 indicate that the roof drift response increases with the increase in the allowable story drift limit of the frame. The (M + SD) roof drift ratios at PGA levels of 0.15 g and 0.6 g are presented in Table 3. The level of 0.15 g represents the design PGA of the frames, while the level of 0.6 g represents the maximum PGA level considered in the analysis.

Table 3 (M + SD) roof drift ratios at PGA levels of 0.15 g and 0.6 g.

Design case	Maximum roof drift ratio (%)	
	PGA = 0.15 g	PGA = 0.6 g
D_1	1	3.28
D_2	1.36	4.62
D_3	1.41	4.92

The results presented in Table 3 indicate that, at PGA level of 0.15 g, the design cases D_2, D_3 exhibited (M + SD) roof drift ratios which are 36% and 41%, respectively, higher than that of the D_1 case.

Fig. 8 shows the relationships between the (M + SD) maximum story drift ratios and the PGA of the earthquakes. The results presented in Fig. 8 indicate that the maximum story drift response increases with the increase in the allowable story drift limit of the frame. The distribution of maximum story drift ratios along the frame stories corresponding to 0.15 g and 0.6 g is shown in Fig. 9(a) and (b), respectively. At 0.15 g the maximum story drift ratio occurred in the 6th story for all the design cases while at 0.6 g the maximum story drift ratio occurred in the 1st story in case D_1, in the 5th story in case D_2 and in the 2nd story in case D_3. The results of Fig. 9 indicate that the design cases D_2 and D_3 exhibit much higher levels of story drifts in comparison with the D_1 case. The (M + SD) maximum story drift ratios at PGA levels of 0.15 g and 0.6 g are presented in Table 4. The results presented in Table 4 at 0.15 g indicate that the design cases D_2, D_3 displayed (M + SD) maximum story drift ratios which are 64% and 54%, respectively, higher than that of the D_1 case. However, the story drift levels obtained in this study for the three design cases at the design PGA level are below the 2.5% maximum story drift ratio specified by FEMA-356 [13] as a life

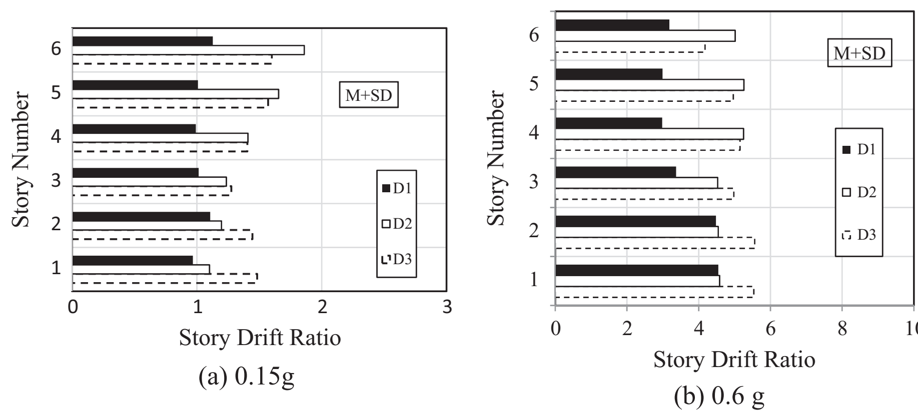

Figure 9 Height-wise distribution of the (M + SD) maximum story drift ratios of the three design cases.

Table 4 (M + SD) maximum story drift ratios at PGA levels of 0.15 g and 0.6 g.

Design case	Maximum story drift ratios (%)	
	PGA = 0.15 g	PGA = 0.6 g
D_1	1.2	4.82
D_2	1.97	5.9
D_3	1.85	6

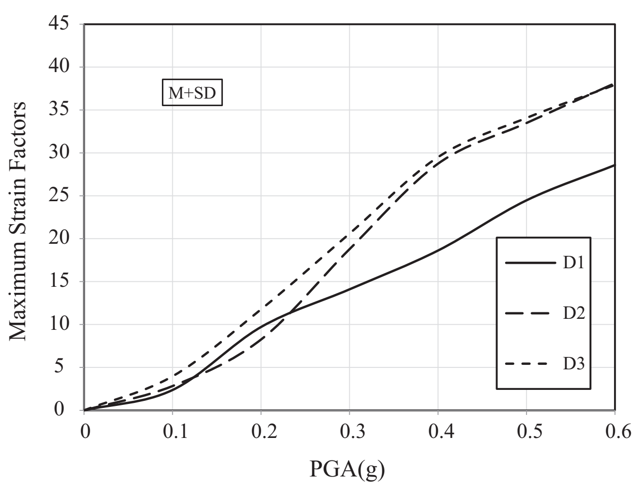

Figure 10 Relationships between the PGA and the (M + SD) maximum column-strain-factor.

safety performance level for earthquake with 10% probability of being exceeded in 50 years which is equivalent to the design earthquake.

Fig. 10 shows the relationships between the (M + SD) maximum column strain factor and the PGA of the earthquakes. The results presented in Fig. 10 indicate that the maximum column strain factor increases with the increase in the allowable story drift limit of the frame. The distribution of column strain factors along the frame stories corresponding to 0.15 g and 0.6 g is shown in Fig. 11(a) and (b), respectively. At 0.15 g and 0.6 g the maximum column strain factors occurred in the 6th story for all the design cases. The (M + SD) maximum column strain factors at PGA levels of 0.15 g and 0.6 g are presented in Table 5. The results presented in Fig. 11 and Table 5 indicate that cases D_2 and D_3 exhibited higher levels of maximum column strains than that of the D_1 case.

Fig. 12 shows the relationships between the (M + SD) maximum beam strain factor and the PGA of the earthquakes. The distribution of beam strain factors along the frame stories corresponding to 0.15 g and 0.6 g is shown in Fig. 13 (a) and (b), respectively. At 0.15 g the maximum beam strain factors occurred in the 4th story in cases D_2 and D_3 and in the 5th story in the D_1 case. At 0.6 g, the maximum beam strain factors occurred in the 1st story in all the design cases. The (M + SD) maximum beam strain factors at PGA levels of 0.15 g and 0.6 g are presented in Table 6. The results presented in Fig. 13 and Table 6 indicate an increase in the levels of maximum beam strains of cases D_2 and D_3 in comparison with that of the D_1 case.

6. Displacement results versus the displacement design limits

The (M + SD) maximum story drift ratios at the design PGA level of 0.15 g are presented in Table 4. The three design cases D_1, D_2 and D_3 exhibited (M + SD) maximum story drift ratios of 1.2%, 1.97% and 1.85%, respectively. These levels of maximum story drift ratios correspond to the strong earthquake case. For the case of moderate frequent earthquake, the displacement demand is estimated by reducing the strong-earthquake displacement to account for the difference in return periods between the strong earthquake and the frequent one. ECP-201 uses a displacement reduction factor v for this purpose. The value of the displacement reduction factor v is 0.4 for important structures and 0.5 for ordinary buildings. This indicates that the (M + SD) maximum story drift ratios corresponding to moderate frequent earthquake are 0.6%, 0.99% and 0.93% for the design cases D_1, D_2 and D_3, respectively.

The allowable maximum story drift ratios for the design cases D_1, D_2 and D_3 are 0.5%, 0.75% and 1.0%, respectively. This shows that case D_3 satisfies the code requirements, while cases D_1 and D_2 exhibit maximum story drift ratios that are

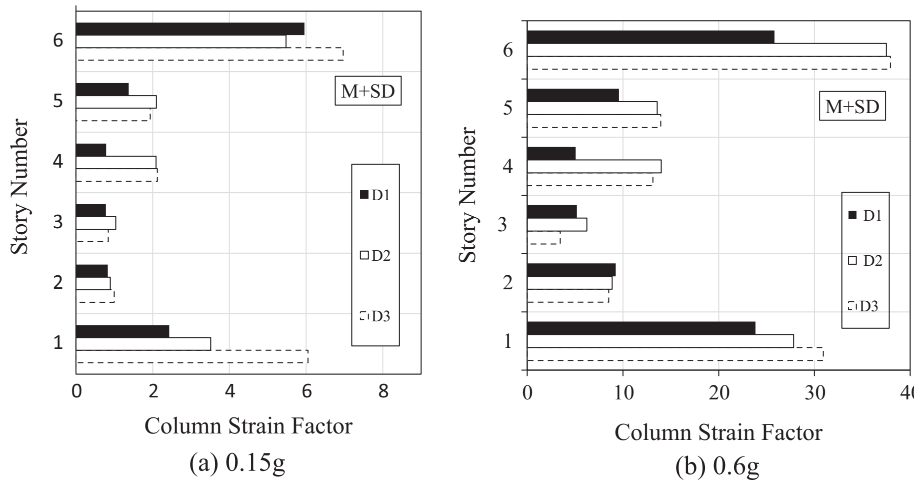

Figure 11 Height-wise distribution of the (M + SD) maximum column strain factors of the three design cases.

Table 5 (M + SD) maximum column strain-factors at PGA levels of 0.15 g and 0.6 g.

Design case	Maximum column strain-factors	
	PGA = 0.15 g	PGA = 0.6 g
D_1	6	28.5
D_2	5.4	38.1
D_3	7.9	37.9

Table 6 (M + SD) maximum beam strain-factors at PGA levels of 0.15 g and 0.6 g.

Design case	Maximum beam strain-factors	
	PGA = 0.15 g	PGA = 0.6 g
D_1	2.70	19.97
D_2	4.5	24.62
D_3	4.80	24.17

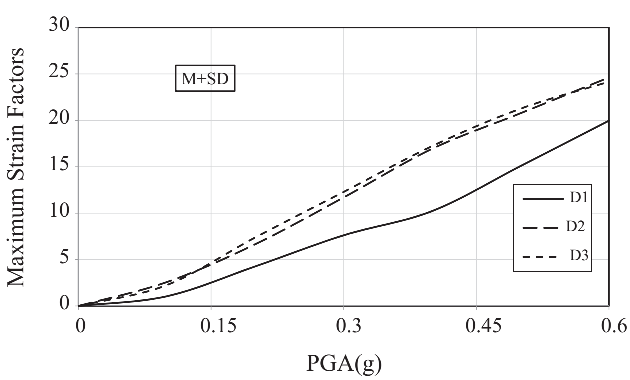

Figure 12 Relationships between the PGA and the (M + SD) maximum beam-strain-factors.

20% and 32%, respectively, higher than the allowed limits specified by the ECP-201.

7. Conclusion

Based on the analysis conducted by this study, the following conclusions can be drawn:

(a) The strength and the initial stiffness of the designed MRSFs decrease as the allowed story drift limit of the frame increases.

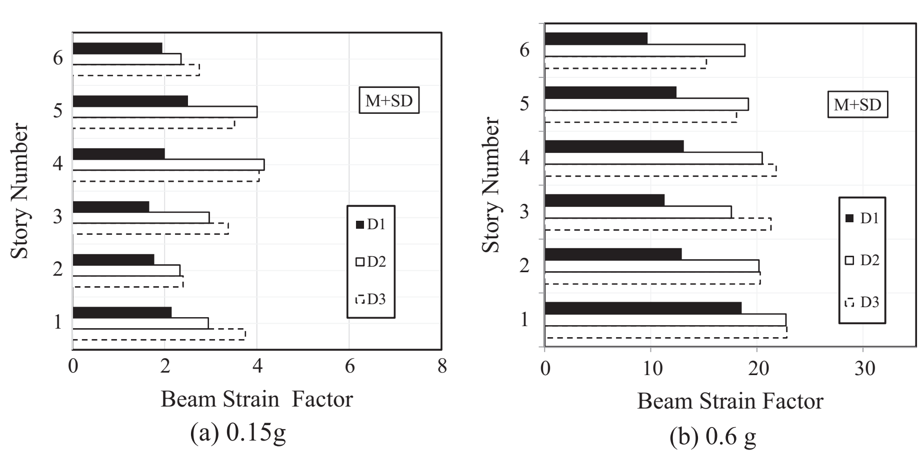

Figure 13 Height-wise distribution of the (M + SD) maximum beam strain factors of the three design cases.

(b) The maximum story drift response of the designed frames under the earthquake loading increase with the increase in the allowable story drift limits. At the design PGA level (0.15 g), the maximum story drifts of the designed frames with 0.75% and 1.0% allowed story drifts are 64% and 54%, respectively, higher than that of the design case with 0.5% allowed story drifts. This trend may be attributed to the fact that the frame strengths decrease with the increase in the allowable story drifts.

(c) The levels of maximum story drifts of the three designed frames at the design PGA are below the 2.5% maximum story drift ratio specified by FEMA-356 [13] as a life safety performance level for earthquake with 10% probability of being exceeded in 50 years.

(d) Under the earthquake loading, the maximum strain response of the MRSF beams increase with the increase in the allowable story drift limits. At the design PGA level (0.15 g), the maximum beam-strain of the designed frames with 0.75% and 1.0% allowed story drifts are 67% and 78%, respectively, higher than that of the design case with 0.5% allowed story drifts. This behavior may also be attributed to the decrease in frame strengths with the increase in the allowable story drifts.

(e) The designed frame with 1.0% allowed story drift satisfies the code requirements with respect to the maximum story drift, while the other design cases with 0.5% and 0.75% allowed story drifts exhibit maximum story drift ratios that are 20% and 32%, respectively, higher than the allowed limits specified by the ECP-201.

It should be noted that the conclusions drawn by this study are based on one building and ten earthquake records. More analysis is required on buildings having different heights and with more earthquake records to achieve more reliable conclusions.

References

[1] ECP-201, Egyptian Code for Calculating Loads and Forces in Structural Work and Masonry, Housing and Building National Research Center, Ministry of Housing, Utilities and Urban Planning, Cairo, 2012.

[2] M.R. Shehata, G.A. Al-Saadi, H. Abou-Elfath, E.A. El-Hout, Push over static analysis of moment resisting steel frames, in: Sixth Alexandria International Conference on Structural and Geotechnical Engineering, AICSGE 6, Alexandria, Egypt, 2007, pp. ST133–ST149.

[3] M.H. Serror, M.M. Hassan, S.A. Mourad, Towards a boundary between special and ordinary steel moment resisting frames in the Egyptian code, in: Proc. of 14th European Conference on Earthquake Engineering, Paper 197, Ohrid, 2010.

[4] E. Mashaly, M. El-Heweity, H. Abou-Elfath, M. Osman, Behavior of four-bolt extended end-plate connection subjected to lateral loading, Alexandria Eng. J. 50 (1) (2011) 79–90.

[5] E. Mashaly, M. El-Heweity, H. Abou-Elfath, M. Osman, Finite element analysis of beam-to-column joints in steel frames under cyclic loading, Alexandria Eng. J. 50 (1) (2011) 91–104.

[6] M.A.A. El-Shaer, Effect of earthquake on steel frames with partial rigid connection, J. Eng. Sci., Assiut Univ. 40 (2) (2012) 343–352.

[7] S. Abdel Raheem, Evaluation of Egyptian code provisions for seismic design of moment-resisting-frame multi-story buildings, Int. J. Adv. Struct. Eng. 5 (2013) 1–20.

[8] M.H. Serror, M.N. Abdelmoneam, Seismic performance evaluation of Egyptian code-designed steel moment resisting frames, HBRC J. (2016) (in press).

[9] S.H. ElKassas, M.A. Haroun, Estimation method of inelastic displacement demands of moment resisting frame buildings in moderate seismic zones, in: Proc. of the 2nd Int. Eng. Mechanics and Materials Specialty Conference, Ottowa, Canada, Paper No. EM-056, 2011, 2011.

[10] M.J.N. Priestley, Displacement-based seismic assessment of reinforced concrete buildings, J. Earthquake Eng. 1 (1) (1997) 157–192.

[11] SeismoStruct v7.0 – A Computer Program for Static and Dynamic Nonlinear Analysis of Framed Structures, 2014. <http://www.seismosoft.com>.

[12] ECP-205: Egyptian Code of Practice for Steel Construction, Load and Resistance Factor Design (LRFD), Housing and Building National Research Center, Ministry of Housing, Utilities and Urban Planning, Cairo, 2008.

[13] FEMA 356, Prestandard and Commentary for the Seismic Rehabilitation of Buildings, Federal Emergency Management Agency, Washington, DC, USA, 2000.